JOURNAL OF GEOPHYSICAL RESEARCH, VOL. 100, NO. D6, PAGES 11,447–11,464, JUNE 20, 1995

Empirical model of global soil-biogenic NO_x emissions

J. J. Yienger and H. Levy II

Geophysical Fluid Dynamics Laboratory/NOAA, Princeton University, Princeton, New Jersey

Abstract. We construct a global, temperature and precipitation dependent, empirical model of soil-biogenic NO_x emissions using 6-hour general circulation model forcing. New features of this source relative to the latest published ones by Dignon et al. [1992] and Muller [1992] include synoptic-scale modeling of "pulsing" (the emissions burst following the wetting of a dry soil), a biome dependent scheme to estimate canopy recapture of NO_x, and an explicit linear dependence of emission on N fertilizer rate for agricultural soils. Our best estimate for annual above-canopy emissions is 5.5 Tg N (NO_x) with a range of 3.3-7.7 Tg N. Globally, the strongest emitters are agriculture, grasslands, and tropical rain forests, accounting for 41%, 35%, and 16% of the annual budget, respectively. "Pulsing" contributes 1.3 Tg N annually. In temperate regions, agriculture dominates emission, and in tropical regions, grassland dominates. Canopy recapture is significant, consuming, on average, possibly 50% of soil emissions. In temperate regions, periodic temperature changes associated with synoptic-scale disturbances can cause emission fluctuations of up to 20 ng N m^{-2} s^{-1}, indicating a close correlation between emission and warm weather events favorable to O_3/smog formation. By the year 2025, increasing use of nitrogen fertilizer may raise total annual emissions to 6.9 Tg N with agriculture accounting for more than 50% of the global source. Finally, biomass burning may add up to an additional 0.6 Tg N globally by stimulating emissions for a short period after the burn.

1. Introduction

The oxides of nitrogen play a crucial role in tropospheric chemistry. NO_x ($NO + NO_2$) is directly linked to the oxidizing efficiency of the troposphere by regulating the concentration of ozone (O_3) and hydroxyl radicals (OH) [*Levy*, 1971; *Chameides and Walker*, 1973; *Crutzen*, 1974, 1979]. Photooxidation of CH_4 and CO, in the presence of elevated NO_x levels (>10-30 parts per trillion - by volume (pptv)), is predicted to produce ozone, and subsequently, OH radicals [*Fishman et al.*, 1979; *Chameides et al.*, 1987; *Lin et al.*, 1988]. Elevated levels of these oxidants, as well as HNO_3 from the direct photochemical oxidation of NO_x, cause numerous environmental problems, including lake acidification, forest diebacks, crop damage, and human respiratory distress [*National Academy of Sciences*, 1983, 1991]. Clearly, we must understand the global budget of this important trace gas.

Presently, there are six recognized sources of tropospheric NO_x: fossil fuel combustion, soil-biogenic emission, biomass burning, lightning discharge, upper troposphere aircraft emission, and stratospheric injection. In order of importance, fossil fuel combustion emits >20 Tg N/yr [*Logan*, 1983; *Hameed and Dignon*, 1988; *Levy and Moxim*, 1989]; soil-biogenic emissions and biomass burning contribute 4-20 Tg N/yr [*Hao et al.*, 1990; *Davidson et al.*, 1991; *Levy et al.*, 1991]; lightning, although published estimates had ranged up to 100 Tg N/yr, is now thought to contribute less than 10 Tg N/yr [*Penner et al.*, 1991; *Lawrence et al.*, 1993] and *Moxim et al.* [1994] have determined an upper limit of 6 Tg N/yr; and the last two are small, contributing less than 1 Tg N/yr [*Levy et al.*, 1980; *Kasibhatla et al.*, 1991; *Kasibhatla*, 1993]. The fossil fuel source, which is both strong and localized, dominates the NO_x budget in industrialized areas [*Logan*, 1983; *Chameides et al.*, 1994]. In rural areas, however, soil-biogenic emissions of NO_x account for a larger fraction of the total NO_x source and may even dominate in remote tropical and agricultural areas. Because of a growing awareness of the importance of soil-NO_x, there is a wide array of published emission data from grasslands, woodlands, savannas, forests (coniferous, deciduous, drought-deciduous, and tropical rain), wetlands, and fertilized soils, taken in North and South America, Africa, Europe, and Australia [see *Williams et al.*, 1992a for an extensive discussion]. The only continent without published soil-NO_x measurements is Asia, which unfortunately includes the vast and heavily fertilized croplands of China and the former USSR.

As part of a continuing effort at the Geophysical Fluid Dynamics Laboratory (GFDL) to understand, quantify, and simulate the global NO_x sources, we develop an empirical model of soil-biogenic NO_x emissions by relating emission to biome, soil temperature, precipitation, and fertilizer application. Developed with a global data set, these relationships provide reasonable means to estimate emissions by filtering out data aberrations observed at individual sites, and subsequently allow the reasonable prediction of emissions in regions with few or no data. We intend to use this source in future chemical transport experiments with the GFDL global chemistry transport model (GCTM) to examine the role of soil-NO_x in atmospheric chemistry.

Paper number 95JD00370.
0148-0227/95/95JD-00370$05.00

2. Background

Building a global soil-NO_x source is in no way easy; emissions are highly variable, both temporally and spatially,

and depend upon a plethora of parameters, including soil temperature, soil moisture, soil nutrients, vegetation cover, N mineralization rates, nitrification/denitrification rates, and others as yet unknown. Initially, to estimate global source strength, researchers assumed data from one or two sites were representative of all land area, resulting in a range of 1-20 Tg N/yr [*Galbally and Roy*, 1978; *Slemr and Seiler*, 1984; *Davidson et al.*, 1991]. As an improvement, researchers developed emission models by empirically relating emission to biome type, soil temperature, and precipitation [*Williams et al.*, 1987, 1992b; *Dignon et al.*, 1992; *Muller*, 1992]. So far the strongest correlations observed are between flux, biome, and soil temperature in temperate climates [*Williams and Fehsenfeld*, 1991; *Valente and Thornton*, 1993; *Stocker et al.*, 1993]. From extensive field work in the United States, *Williams and Fehsenfeld* [1991] drew two major conclusions: first, for any given temperature, temperate emissions are "stratified" across major biomes (that is, grassland emissions are generally an order of magnitude greater than those of forests, while those of heavily fertilized soils are an order of magnitude greater than those of grasslands); and second, NO emissions in a particular biome can be described with an exponential temperature dependence model:

$$Flux = A \times e^{k[^\circ C^{-1}] \times T} \quad (15 < T < 35) \qquad (1)$$

where T is soil temperature in degrees Celsius, A in ng N m^{-2} s^{-1} is a biome fitting parameter, and k is a dependency coefficient which is relatively constant across biomes. They developed an emission algorithm by averaging the k values from all their field studies and then substituting flux/temperature data into (1) by biome and taking the average of the subsequent set of A values as the "A factor" for that biome. For agriculture, Williams defined A factors for individual crops by experimentally determining A factors for soybeans (average fertilizer rate, 3 kg N/ha) and corn (121 kg N/ha), and then using linear interpolation to define A factors for other crops based on average fertilizer rate. They generated an inventory of U.S. soil emissions by applying monthly averaged temperature fields and a biome/crop classification map to the algorithm. *Muller* [1992] and *Dignon et al.* [1992] used the Williams algorithm on a global scale and estimated emissions of 5-7 Tg N/yr.

For global application, this approach has merit as well as deficiencies. Further research confirms the existence of an exponential temperature dependence but only in nonparched, noninundated soils. In very dry soils, the strong exponential temperature dependence becomes weaker and more linear (or disappears altogether) [*Stocker et al.*, 1993], and at any given temperature, emissions are 3-5 times less than in comparable moist soils [*Johansson and Sanhueza*, 1988; *Levine et al.*, 1993]. In extremely wet or inundated soils, emissions drop owing to the suppression of nitrifying bacteria and/or the clogging of soil pores which ventilate NO to the atmosphere [e.g., *Sanhueza et al.*, 1990]. This moisture dependence can be reasonably neglected in temperate climates, but it must be considered in the tropics where the Intertropical Convergence Zone (ITCZ) migration produces large and prolonged fluctuations in soil moisture. There also appears to be an "optimal" temperature for biogenic processes above which the temperature dependence weakens or disappears. There have been no systematic reports of temperature dependencies in the tropics, and it is theorized that this is because most measurements were taken above this optimal temperature [*Cardenas et al.*, 1993]. Figure 7 of *Valente and Thornton* [1993], which is a plot of NO emissions versus soil temperature in a temperate climate, supports this hypothesis. The data points imply an optimal temperature of ~30°C (most tropical data sites had average soil temperatures over 30°) as they show a particularly strong exponential soil temperature/NO_x flux dependence below 27°C but none at all between 30° and 40°C. Applying (1) above 30°C would systematically overestimate emissions, and given that some tropical environments have soil temperatures well over 45°C, the error would be quite large.

There are four other well-documented phenomena which we will also consider in this study: "pulsing," nitrogen fertilizer stimulation, biomass burning stimulation, and canopy reduction. Each is discussed briefly below.

2.1. "Pulsing"

If a very dry soil is wetted, a large burst, or "pulse," occurs and then decays rapidly over a period of time following the wetting event. Typically, the pulse flux begins at 10-100 times the background level and decays over a period of a few days to a few weeks, depending upon the severity of the antecedent dry period and the amount of precipitation [*Stocker et al.*, 1993; *Valente and Thornton*, 1993; *Williams et al.*, 1987; *Williams and Fehsenfeld*, 1991]. It is thought to be caused by a release of built-up inorganic N trapped on the dry soil and a concurrent reactivation of water stressed bacteria which then metabolize the excess nitrogen [*Davidson et al.*, 1992a; *Davidson et al.*, 1993]. Pulsing occurs as part of a continuous cycle of wetting, drying, and nutrient accumulation, so its exact regional impact varies with local climatology. Presumably the strongest impact is in the tropics, where there are extended dry seasons followed by wet seasons. The simultaneous wetting of large tracts of dry soils may produce a brief "flux season" in which cumulative emissions are larger than those from the entire dry season. *Davidson et al.* [1991] confirmed this in a Mexican pasture and drought-deciduous forest, where pulses at the beginning of the wet season accounted for 8-20% of the annual emissions, whereas dry season fluxes cumulatively accounted for only 4-10% of the annual budget. The first large-scale observations of dry-to-wet season pulsing were made recently in Africa, where researchers observed very strong emissions (20-40 ng N/m^2 s) from a 100-km^2 area of savannas at the beginning of the wet season [*Harris et al.*, 1993].

2.2. Nitrogen Fertilizer Stimulation

It is well established that adding N fertilizers to soils increases biogenic NO_x emission [e.g., *Shepard et al.*, 1991]. A number of researchers found emission rates from fertilized soils rivaling those found in urban areas from combustion [e.g., *Williams et al.*, 1988]. The mechanisms attributed to this are enhanced biological nitrification and denitrification, depending on the form of the fertilizer (either ammonium or nitrate). Exactly which form is more stimulatory depends on the site, although evidence suggests that a mixed form, such as NH_4NO_3, generates strongest emission [*Sanhueza*, 1992]. Field response to fertilization is variable; some plots have enhanced emissions for prolonged periods, whereas others have sharper initial increases that decay over time. In general, however, there appears to be a positive linear correlation

between fertilizer use and emission, and over the course of a growing season, total emissions translate into 1-10% of added nitrogen fertilizer (see Table 1) [*Williams et al.*, 1992b; *Shepard et al.*, 1991; *Cardenas et al.*, 1993; *Matson et al.*, 1993]. This magnitude of loss indicates potentially strong emissions in areas with heavy fertilizer use such as the northern hemisphere "Metro-Agro-Plexes" (MAPs) (Eastern North America (25°-50°N, 150°-60°W), Europe/Russia (36°-70°N, 10°W-90°E), and Eastern China and Japan (25°-45°N, 100°-146°E)), highly compact regions of anthropogenic activity which account for 75% of the world's industrial and agricultural productivity [*Chameides et al.*, 1994]. Although NO_x pollution in the MAPs is due mainly to fossil fuel combustion, it is possible that soil-NO_x dominates over the regions of intensive agriculture during the summer when soil emissions are at a maximum.

2.3. Biomass Burning Stimulation

Preliminary evidence suggests that biomass burning may enhance soil emissions by a factor of 5-10 for several weeks following the burn [*Johansson et al.*, 1988; *Anderson et al.*, 1988]. Investigations of preburn and postburn soil nutrients revealed that burning has a "fertilizing" effect by raising ammonium levels [*Levine et al.*, 1990]. If emissions are systematic for all burning, they will be most affected in tropical savannas, because a majority of annual burning occurs there [*Menaut et al.*, 1991]. Furthermore, in the tropics, burning stimulation can compound pulsing and seasonally skew strongest emissions to the transition period between dry and wet seasons. Each year, approximately 40% of the savannas are burned toward the end of the dry season to make way for new growth, while at the same time, the first rains of the wet season are stimulating bacterial activity and releasing nitrogen accumulated during the dry season. Measurements in Africa showed that dry savannas, which were burned and then wetted, had higher emissions than those which were just burned or wetted [*Levine et al.*, 1993].

2.4. Canopy Reduction

Before escaping the plant canopy, some of the NO_x is lost by a process we refer to as "canopy reduction" (CR). CR is a combination of losses resulting from diffusion of NO_2 through plant stomata and direct deposition of NO_2 onto and through the cuticle [*Hanson and Lindberg*, 1991]. During the daytime the former effect is dominant, but during the night, when the stomata are closed, the latter effect is amplified, because NO_2 is more abundant at night and because canopy residence times are generally longer in the more stable nighttime [*Jacob and Bakwin*, 1991]. By either mechanism, the loss rate of NO (which is actually the dominant component of soil-NO_x emission) is much smaller than NO_2, so one might suspect that net CR is small. However, a significant portion of the NO is converted (by reaction with O_3) within the canopy into NO_2, leading to an estimated 75% removal efficiency in tropical rain forests [*Jacob and Wofsy*, 1990].

A soil-NO_x source which is fit from field data must include a parameterization for CR, because the most frequently used data collection techniques, the gradient and chamber methods [e.g., *Parrish et al.*, 1987], measure emissions only from the soil surface. In the gradient technique, the NO flux is measured by sampling the concentration of NO and O_3 at different levels above the soil and then, assuming the only sink for NO is the conversion to NO_2 by O_3, integrating that rate equation through height and solving for the initial condition (the soil flux). Although this method is accurate for determining the initial output of NO at the soil surface, it is inappropriate for estimating flux escape from the canopy because the fate of the ensuing NO_2 remains unknown. It is reasonable to assume that at least a portion of it will be deposited on the plant canopy, and thus contribute to a reduction in the net flux. The chamber (or enclosure) methods pose a similar problem. In most cases, an opaque chamber is initially flushed with zero air to clean out any ambient NO_x and ozone, and then the NO flux is assumed to be proportional to the rate of buildup within the chamber. This rate is observed to be closely linear, because the concentrations of NO_2 and O_3 within the chamber drop to near zero after 1-2 min owing to rapid deposition and because the opaque walls prevent further photochemical activity [e.g., *Williams et al.*, 1987]. The absence of an NO to NO_2 mechanism within the chamber removes a potential sink for emitted NO, the NO_2 deposition on the canopy. Since this would occur (quite rapidly) outside the chamber, measurements made with this technique can only be considered net NO emission from the soil, and not an actual input of NO_x to the atmosphere above the canopy.

Table 1. N Fertilizer Loss Rates as NO_x

Reference	Period	% loss
Hutchinson and Brams [1992]	9 weeks	3.2
Williams et al. [1992b]*	4 weeks	2.8†
Valente and Thornton [1993]	15 weeks	2.5†
Shepard et al. [1991]	26 weeks	11.0
Slemr and Seiler [1984]	4 weeks	2.7
Slemr and Seiler [1991]	3 weeks	0.06-0.21
Anderson and Levine [1987]	52 weeks	0.8
Johansson et al. [1988]	30 hours	0.5

* Obtained by integrating Williams algorithms using FAO fertilizer data for the United States.

† Net emissions from field divided by applied fertilizer.

3. Approach

In this paper we present an empirical global source based on Williams's temperature dependence approach but with modifications and additions to account for all aforementioned phenomena. Main features include separate exponential temperature dependence for wet soils and linear dependence for dry soils, an optimal temperature above which flux becomes temperature independent, scalar adjustments to account for both "pulsing" and canopy reduction, synoptic-scale temperature and precipitation forcing, an explicit linear dependence of emission on fertilizer rate, and finally, a crude scheme to simulate biomass burning stimulation of emissions. Because of the empirical nature of the source, we only intend it as a "best estimate" based on available data. No doubt there

will be discrepancies between this work and future soil-NO_x measurements, since we rely on extrapolation of a complex process with a limited number of parameters.

Albeit not an exact representation of soil-NO_x emission, there are several uses for this source. By capturing well-established emission differences between biomes, photochemical transport models can access the potentially strong impact of, say, fertilized soils relative to lower-emitting grasslands and forests. *Chameides et al.* [1994] used a version of this source in a model with simple nitrogen chemistry, in conjunction with an empirical estimation of O_3 pollution [*Trainer et al.*, 1993], to predict the role of N fertilizers in crop damage by O_3. With synoptic-scale climate forcing, we can investigate a possible correlation between emission and events favorable for smog/O_3 formation, such as warm summertime high-pressure systems. The "pulsing" scheme and moisture-variable temperature-dependent emission should capture the important role of soil moisture in tropical soil-NO_x emissions. For example, previous inventories that excluded the effects of soil moisture were unable to account for the large differences between dry and wet season emissions and the pulsing that occurs at the transition (dry to wet). In a nonquantitative application, we can identify regions where further field research would be fruitful, i.e., regions that may have high emissions but lack field data to back up that conclusion. We address many of the above points in case studies described later.

4. Source Construction

We start by identifying global biomes that either are expansive or have enough supporting emission data to warrant separate classification. These include water, ice, desert, tundra, grassland, scrubland, woodland, deciduous forests, coniferous forests, drought-deciduous forests, rain forests, and agricultural lands. Of these, water, ice, desert, and scrubland are assumed to have no emission. The remaining biomes are mapped out on a 1° × 1° grid using a simplified version of the 36-type NASA/Goddard Institute for Space Studies (GISS) Global Vegetation Index [*Mathews*, 1983; *Mathews*, 1985]. Table 2 identifies which NASA/GISS classifications we group under each biome. Agriculture was presented as an overlying grid with cultivation percentages defined for each grid box. We scaled these percentages so that the agricultural area in each country would reflect statistics from the Food and Agricultural Organization of the United Nations (FAO). This reduced the NASA/GISS global agricultural area from 1.75×10^{13} to 1.41×10^{13} m^2.

Table 2. Mathews Categories Grouped Under Each Biome

Biome	Mathews Index
Water	-
Ice	V
Desert	U
Scrubland	H,I,J,K,L
Tundra	M,T
Grassland	N,O,P,Q,R,S
Woodland	C,D,E,F,G
Deciduous forest	A,B
Coniferous forest	4,5,6,8
Drought deciduous forest	9
Rain forest	1,2,3,7

The empirical relationships used to compute emission are of the form

$$Flux = f_{w/d}(\text{soil temperature}, A_{w/d}(\text{biome})) \times P(\text{precipitation}) \times CR(LAI, SAI) \quad (2)$$

where $f_{w/d}$(soil temperature, $A_{w/d}$(biome) is some function either constant, linear, or exponential and $A_{w/d}$(biome) is a coefficient used to distinguish between biomes. The subscript *w/d* stands for the soil moisture state, either "wet" or "dry" (see section 2.1 for our definition of the two soil moisture states). *P*(precipitation) is a scalar factor used to adjust the flux in the event of a pulse (see section 2.1), and *CR*(*LAI*, *SAI*) is a scalar reduction factor that accounts for uptake of NO_x by the plant canopy (see section 2.4).

We calculate emissions every 6 hours for 1 year, using temperature and precipitation fields from a parent general circulation model (GCM) [*Manabe et al.*, 1974]. We require GCM data because synoptic-scale observed temperature and precipitation data are not readily available and this time resolution is required to drive our pulsing scheme, estimate soil moistures, and reduce the systematic underestimation caused by applying long-term averaged data to a nonlinear temperature/NO_x flux relationship. Although the GCM does not have diurnal insolation and cannot realistically simulate atmospheric fluctuations with time scales less than 6 hours or spatial scales less than 300 km, it does generate synoptic-scale features of the Earth's climate such as transient midlatitude cyclones [*Manabe and Holloway*, 1975]. It is also reliable for simulating the migration of the ITCZ [*Manabe et al.*, 1974], a particularly valuable feature because we find that associated long-term wetting and drying in the tropics is the major source of pulsing emissions.

Our emission model requires soil temperatures not readily obtainable from the GCM. The "surface temperatures" carried in the GCM do not include biome parameterization and therefore cannot account for the large effect vegetation has on soil temperature. Instead, we convert the lowest model level air temperatures to soil temperatures as follows: In wet soils we use the empirical relationships derived by *Williams et al.* [1992b], and in dry soils we add 5°C to the model temperature, based on observations of *Johansson et al.* [1988]. Although some may argue that adding only 5° to dry soils is overly conservative, we will show later that dry soils, regardless of the temperature, are relatively insignificant in the global budget. Below, we present the derivation of each component in (2).

4.1. Pulsing, *P*(Precipitation)

After every 6-hour interval, we define the grid box soil moisture as either "wet" or "dry" to determine whether or not to allow pulsing at the next time step. We consider a soil "dry," in the sense that it will pulse when wetted, if it receives less than 1 cm of precipitation in the previous 2 weeks. This precipitation rate, typical of tropical dry seasons, implicitly parameterizes the meteorological conditions required for

pulsing (i.e., some combination of dryness and nutrient buildup). For the lack of better data, we use this "dry" criterion year-round and over the whole globe, conceding that it definitely varies with climate (particularly with soil temperature). Also, implying a spatially independent rate of nutrient buildup rate ignores the fact that soils in close proximity to industrial centers receive more N deposition than those in remote locations [*Levy and Moxim*, 1989]. A more sophisticated method might be to use a GCM "bucket" hydrology to determine when a soil is dry and then define a regional time period required for sufficient nutrient buildup to cause a pulse. Unfortunately, not enough observations are available to define pulsing in such a framework. Our "dry season rate" method is simple, but at least we know for sure that this time scale and precipitation rate, based on the numerous observations of pulses following dry seasons, are conducive to pulsing.

In our model, a pulse will occur if a dry grid box receives sufficient rainfall. To parameterize the required rainfall, as well as the pulse's magnitude and duration, we rely on qualitative fitting to experimentally documented pulses. During a pulse in the Venezuelan savanna (after a 2.3-cm rainfall), the soil moisture dropped from a relatively high 15% to 2% after 17 rainless days, and this drying period correlated well with the length of the pulse [*Johansson and Sanhueza*, 1988]. The pulse from a lessor amount of water, 1.2 cm, applied to a dry savanna soil lasted less than 1 week, decreasing exponentially [*Johansson et al.*, 1988]. Even a tiny amount of rain, 0.03 cm, applied to a dry grassland soil caused an immediate fivefold to tenfold jump in emission, which then decayed rapidly over 2 days [*Williams et al.*, 1987]. On the basis of these and other similar observations reported in the literature, we developed a simple four-step pulse scheme based on daily cumulative precipitation.

Rain Rate, cm/day	Pulse Description
< 0.1	no pulse (assume evaporation)
0.1 < rain < 0.5	"sprinkle," a 3-day pulse starting × 5 with exponential decay
0.5 < rain < 1.5	"shower," 1-week pulse starting at × 10 with exponential decay
1.5 < rain	"heavy rain," 2-week pulse starting at × 15 with exponential decay

We chose exponential decay because pulsing is correlated with soil drying [*Sanhueza*, 1992; *Stocker et al.*, 1993], and under ideal situations (i.e., constant sun, temperature, and relative humidity), soil moisture would decrease exponentially (A. Broccoli, private communication, 1994). Fitting exponential curves to these parameters, we get P(precipitation):

No pulse

$$P(\text{precipitation}) = 1.0 \quad (3)$$

"Sprinkle"

$$P(\text{precipitation}) = 11.19 \times e^{-0.805\,[day^{-1}] \times t} \quad (1 < t < 3) \quad (4)$$

"Shower"

$$P(\text{precipitation}) = 14.68 \times e^{-0.384\,[day^{-1}] \times t} (1 < t < 7) \quad (5)$$

"Heavy rain"

$$P(\text{precipitation}) = 18.46 \times e^{-0.208\,[day^{-1}] \times t} (1 < t < 14) \quad (6)$$

where t is days, with the pulse beginning at $t = 1$ and counting up through its duration. These functions provide scalar factors (between 1 and 15) which are applied directly in (2). There can be no pulse initiation in a "wet" soil but if the pulse-causing rain is substantial enough to change the moisture state from dry to wet, or if the moisture state changes amidst a pulse, then the pulse will still occur (or continue) and decay uninterrupted as described by (4), (5), or (6).

4.2. Temperature Dependencies, $f_{w/d}$(*Soil Temperature*, $A_{w/d}$(*Biome*))

As discussed in section 2, the soil temperature/flux dependence diminishes from exponential to linear with decreasing soil moisture. Because of a dearth of data, we are unable to explicitly include soil moisture in a soil temperature/flux relationship; however, we can fit a separate exponential form for "wet" soils and linear form for "dry" soils. We must point out that the "wet" category includes inundated soils and that we neglect the possibility that saturation decreases emissions (except for a simple implicit treatment in tropical rain forests and rice fields to be described later) because this state is presently too difficult to resolve on a global scale. This omission might cause a slight overestimate of emissions, but the error should be minimal because high evaporation rates in non-rain forest tropical biomes (i.e., most error would be during the tropical savanna wet season) routinely drop soil moistures to as low as 2%, even during the wet season [*Johansson and Sanhueza*, 1988].

4.2.1. Wet soils. We define f_w(soil temperature, A_w(biome)) for three soil temperature intervals, cold-linear (0-10°C), exponential (>10-30°C), and optimal (>30°C), as

$$0.28 \times A_w(\text{biome}) \times T \quad (7a)$$

$$f_w(T, A_w(\text{biome})) \left[\frac{\text{ng N}}{\text{m}^2\text{s}}\right] = A_w(\text{biome}) \times e^{(0.103 \pm 0.04) \times T} \quad (7b)$$

$$21.97 \times A_w(\text{biome}) \quad (7c)$$

where A_w(biome) is the "wet" biome coefficient analogous to the A in (1) and T is soil temperature in degrees Celsius. Following an approach similar to the one used by *Williams et al.* [1992b] to develop their U.S. inventory, we assume emissions from wet soils (as opposed to all soils in the Williams inventory) between 10° and 30°C are characterized by (1) and that k is constant globally. The weighted average k (0.103 ± 0.04 one sigma) of the data in Table 3, which shows all reported exponential temperature dependencies, yields a general dependence. The range of 10-30 corresponds to the range at which all dependencies in Table 3 were consistent. For temperatures between 0° and 10°C, we derived a simple "cold-linear" relationship between the flux computed by the exponential at 10° and zero flux at 0°C. For temperatures above 30°, we defined a temperature independent "optimal" flux as the flux computed by the exponential at 30° (in (7c),

Table 3. Exponential Temperature Dependencies of Moist Soils From Various Biomes

Site	Number of Points	T °C, Dependence
Winter wheat[a]	66	0.11 ± 0.01
Grassland (NO_y)[b]	12	0.10 ± 0.02
Deciduous forest[c]	98	0.076
Corn field[c]	144	0.130
Pasture[c]	122	0.189
Grassland[d]	46	0.068 ± 0.02
Grassland[d]	43	0.056 ± 0.03
Deciduous forest[d]	32	0.040 ± 0.05
Deciduous forest[d]	52	0.130 ± 0.13
Coastal marine[d]	30	0.052 ± 0.04
Corn field[d]	89	0.066 ± 0.05
Wheat field[d]	119	0.073 ± 0.01
Weighted average		0.103 ± 0.04

The T dependence is the slope of the ln (flux) versus soil temperature.

[a] Data from Anderson and Levine [1987] computed by Stocker et al. [1993].

[b] Stocker et al. [1993].

[c] Valente and Thornton [1993].

[d] Williams et al. [1992b].

21.97 is merely the exponential term with 30°C substituted in for temperature). Below 0°, we assume emissions are zero because they are insignificant for the purposes of this global source.

A_w(biome) coefficients are calculated for each biome (except for rain forests and agricultural soils) by applying available mean soil temperature and NO_x flux data to (7a-c) and taking the mean of the subsequent set of ln (A_w(biome)) values. We use logarithmic averaging to reduce the effect of extreme values. All of the wet soil data, as well as the calculations of A_w(biome) values, are presented in Table 4.

For agricultural soils, we make A_w(agriculture) linearly depend on N fertilizer rate and constrain it to force a 2.5% loss of applied N fertilizer annually per grid box:

$$A_w(\text{agriculture})\left[\frac{\text{ng N}}{\text{m}^2\text{s}}\right] = A_w(\text{grassland})\left[\frac{\text{ng N}}{\text{m}^2\text{s}}\right] + S \times \text{fertrate}\left[\frac{\text{kg N}}{\text{ha month}}\right] \quad (8)$$

where the "intercept" is A_w(grassland) and the slope S (ng N/ m^2 s/kg N/ ha/month) is calculated for each grid box to force a 2.5% loss of fertilizer. We choose 2.5% because available estimates (shown in Table 1) cluster around this percentage. The monthly fertilizer rates were derived by using FAO statistics of per-country annual fertilizer use, and assuming that all fertilizer is broadcast uniformly during the growing season (defined as May-August for the northern temperate zone (above 30°N), November-February for the southern temperate zone (below 30°S), and year-round for the tropics (30°N-30°S)). We assume that fertilization elevates soil nitrogen to constant levels during the growing season, and that during the off-season, no residual fertilizer remains, so that soils emit as grassland. While not physically true, this assumption is reasonable because off-season croplands have been shown to emit on the same order of magnitude as grassland (see *Williams et al.* [1992b] for a complete emission summary of "not recently fertilized" croplands). We treat all crop types the same with the exception of rice, which emits much less NO_x than other crops because of soil inundation [*Galbally et al.*, 1987]. On the basis of research by *Galbally et al.* [1987], we reduced the fertilizer loss rate and the background emission rate for rice by a factor of 30 and define agriculture in the region 0°-35°N and 80°-140°E to be all rice, and in the region 0°-35°N and 60°-80°E to be one-half rice. The former box covers the main rice-producing areas of southeast Asia and Japan, and the latter box covers the mixed growing region of central and eastern India [*Times Atlas of the World*, 1967].

4.2.2. Dry soils. In dry soils the soil temperature/NO_x flux correlation is weak, if it exists at all. Three of the four researchers who found one [*Johansson et al.*, 1988; *Anderson and Levine*, 1987; *Stocker et al.*, 1993] reported a weak positive linear correlation, while the fourth [*Cardenas et al.*, 1993] reported a stronger negative correlation. This variability prevents any statistically significant general correlation from being obtained. Therefore we define only two temperature regimes for $f_d(T, A_d(\text{biome}))$: cold-linear (0°-30°C) and optimal (>30°C):

$$f_d(T, A_d(\text{biome}))\left[\frac{\text{ng N}}{\text{m}^2\text{s}}\right] = \begin{cases} \dfrac{A_d(\text{biome}) \times T}{30} & (9a) \\ A_d(\text{biome}) & (9b) \end{cases}$$

A_d(biome) is the "optimal" flux, or the average of all fluxes recorded over 30°C, and T is soil temperature in degrees Celsius. The "cold-linear" formulation is analogous to wet soils, except that the upper limit extends to the optimal temperature, thus cutting out the exponential dependence. The slightly positive linear relationship in the 0°-30° range, while not explicitly fit to real data, is at least consistent with three of the four researchers reporting a temperature dependence in dry soils.

Computation of the A_d(biome)s (see Table 5) is difficult because there are only scattered NO_x measurements from dry grasslands (and one from a drought-deciduous forest). For natural biomes without dry data, we use wet emission data divided by three, assuming a moisture dependence consistent with that observed in grasslands. For dry agriculture, we use (7a-c) because emission response to fertilizer in dry soils has not yet been examined and it is very possible that the grassland moisture dependence is not valid in this complex system. If agriculture follows the pattern observed in grassland and has lower "dry" emissions, our parameterization might be considered high during dry periods. However, since we set annual emission as a percentage of the yearly applied fertilizer, this will act only to smooth out emissions over the year and not actually cause an overall increase. Furthermore, it is probable that much of the fertilized dry agricultural land would be irrigated, thus reducing the error.

4.2.3. Tropical evergreen rain forests. Tropical rain forests are unique because researchers report no correlation between temperature and emission, even at temperatures well below 30°C [*Kaplan et al.*, 1988]. Therefore we set $f_{w/d}$(soil temperature, $A_{w/d}$(biome)) constant with respect to soil moisture condition: 8.6 ng N/m^2 s for dry soils and 2.6 ng N/

Table 4. Wet Soil Biome Data

Biome (Reference)	Site	Mean NO_x Flux, (ng N/m^2 s)	Mean Soil Temperature, °C	ln (A_w(biome))	A_w(biome)
Grassland/savanna					
Williams et al. [1987]	Colorado	0.55	8.20	-1.427	
Williams et al. [1991]	Colorado	10.00	27.2	-0.444	
Williams et al. [1987]	Colorado	4.92	23.7	-0.799	
Anderson et al. [1987]	Virginia	3.47	26.2	-1.402	
Delaney et al. [1986]	Colorado	9.00	26.5*	-0.479	
Stocker et al. [1993]	Colorado	7.60 (NO_y)	27.0	-0.700	
Galbally and Roy [1978]	Australia	3.31	19.8	-0.805	
Johansson and Sanhueza [1988]	Venezuela - I	56	>30	0.811	
	Venezuela - II	10	>30	-0.787	
Sanhueza et al. [1990]	Venezuela	0.64	26.8	-3.207	
Davidson et al. [1991]	Mexico				
	upland	28.6	30.0	0.263	
	floodplain	25.6	30.0	0.152	
Cardenas et al. [1993]	Venezuela	4.93	>30	-1.752	
(D. Serca, unpublished data, 1994)	Ivory Coast	0.45	>30	-3.889	
(D. Serca, unpublished data, 1994)	South Africa	5.10	>30	-1.461	
Mean		...	...	-1.022	0.36
Coniferous and deciduous forests					
Williams and Fehsenfeld [1991]	Tennessee	0.31	20.0	-3.231	
Williams et al. [1988]	Pennsylvania	1.20	28.4*	-2.743	
Thornton and Valente [1992]	North Carolina	0.13	24.5*	-4.564	
Thornton and Valente [1992]	Mississippi	0.05	22.5*	-5.448	
Johansson et al. [1984]	Sweden	0.35	15.0*	-2.685	
Johansson et al. [1984]	Sweden	0.23	15.0*	-3.105	
Mean		...	...	-3.531	0.03
Drought deciduous forest					
Davidson et al. [1991]	Mexico	2.02	30.0*	-2.301	
Sanhueza el al. [1990]	Venezuela	0.55	26.8	-3.336	
Mean				-2.283	0.06
Tundra					
Bakwin et al. [1992]	Alaska	0.04	3.0*	-3.528	0.05
Woodland†					0.17

* Site lacked mean temperature data so we used GCM data.

† No field data. A_w(woodland) is average of grassland and coniferous/deciduous forests.

Table 5. Biome Data for Dry Biomes

Biome	Site	Mean Flux (ng N/m^2 s)	Mean Soil Temperature, °C	A_d(biome) (Mean Over 30°)
Grassland/savanna				
Johansson et al. [1988]	Venezuela	8.00	>30	
Williams et al. [1987]	Colorado	1.22	>30	
Cardenas et al. [1993]	Venezuela	3.68	>30	
Davidson et al. [1991]	Mexico	0.09	>30	
Levine et al. [1993]	South Africa	1.50*	>30	
Stocker at al. [1993]	Colorado	4.20 (NO_y)	30.0	
Rondon et al. [1993]	Venezuela	1.30	>30	
(D. Serca, unpublished data, 1994)	Ivory Coast	0.10	>30	
(D. Serca, unpublished data, 1994)	South Africa	3.80	>30	
Mean		2.65		2.65
Drought deciduous forest		0.40	>30	0.40
Coniferous and deciduous forest†				0.22
Tundra†				0.37
Woodland†				1.44

* mean of reported 1-2 ng N/m^2 s range.

† Computed as the optimal flux in wet soils divided by three.

m^2 s for wet soils. These values reflect the average rain forest emissions recorded during the wet and dry season in Venezuela [*Bakwin et al.*, 1990; *Kaplan et al.*, 1988] and Africa (D. Serca, unpublished data, 1994). The apparent inversion with other biomes (that is, greater emissions in the dry season as opposed to the wet season) can be explained by the almost constant soil inundation during the wet season [*Bakwin et al.*, 1990]. The dry season is drier, but still somewhat rainy, and it is probable that the soil moisture only drops to levels considered optimal for NO_x emission, somewhere between 10% and 18% [*Cardenas et al.*, 1993]. If we used our traditional scheme to define soil moisture state in rain forests (defined in section 4.1), we would miss most of the dry season. Therefore we force the model to emit at the dry soil rate for the five contiguous driest months, regardless of the actual model soil moisture state. However, the soil still must meet the requirements defined in section 4.1 in order to pulse.

5. Canopy Reduction, *CR(LAI, SAI)*

Jacob and Bakwin [1991] developed a CR scheme for a Brazilian rain forest site as a function of five key variables: surface O_3, NO soil emission, leaf resistance to deposition, canopy residence time, and leaf area index (LAI). Surface O_3 and NO emission determine the intercanopy NO_2/NO_x ratio, and the other three determine the efficacy of the canopy for NO_2 uptake. This scheme is not yet practical for global inventories because it relies on experimental measurements of vertical transfer rates and NO_2 deposition velocities. Estimating vertical transport with model data (i.e., using an eddy diffusion coefficient as the product of the lowest-level model winds and surface roughness) is possible, but the interaction of the resulting "surface" turbulence and intercanopy turbulence is too complex to parameterize accurately. The only reliable parameters available globally, which are linked to CR, are leaf and stomatal areas. If we explicitly ignore NO_2/NO_x ratio, canopy residence time, and stomatal resistance, we can model the canopy as a simple "gray absorber" of NO_2 dependent only on LAI and the product of LAI and ratio of stomatal area to leaf area (product defined as the stomatal area index (SAI)). LAI and SAI are alternative diagnostics of CR because it is reasonable to assume the amount of NO_x lost in a canopy is roughly dependent on the total leaf (cuticle) and stomatal area. Choosing the exact model form of this dependence is difficult; for simplicity, we use an exponential decay model, assuming that stomata and cuticle absorb a constant fraction of NO_2 they encounter and are distributed uniformly throughout canopy. Then, considering an idealized case of only cuticle absorption at night and stomatal absorption during the day, we define the daily averaged flux escape efficiency, or *CRF(LAI, SAI)* as

$$F_{\text{from-canopy}} = F_{\text{from-soil}} \times \left(\frac{e^{-(k_s \times SAI)} + e^{-(k_c \times LAI)}}{2} \right) = F_{\text{from-soil}} \times CRF\,(LAI, SAI) \quad (10)$$

where k_s and k_c are some "stomata" and "cuticle" absorptivity constants and the term $(e^{-ks \times SAI} + e^{-kc \times LAI})/2$ is applied to (2) as *CR(LAI, SAI)* (heretofore referred to as the canopy reduction factor or CRF). The constants k_s [8.75 m^2/m^2] and

k_c [0.24 m^2/m^2] are computed with *Jacob and Wofsy* [1990] rain forest CR data and average LAIs and SAIs reported by *Barbour et al.* [1987] and *Larcher* [1991], respectively: night, 85% removal, 8 LAI [m^2/m^2]; day, 65% removal, 0.12 SAI [m^2/m^2]. CRFs for all the biomes are presented in Table 6, as well as the seasonal period in which they are applied.

The reader should be aware that this "gray absorber" model is not physically based. The rate of NO_2 consumption is controlled by interstomatal kinetics, which in turn is controlled by stomatal resistance to deposition, NO_2/NO_x partitioning, and vertical transfer rates. We do have an implicit dependence on canopy residence time, and hence vertical transfer rate, through our use of LAI because it can be argued that the two are closely dependent (D.J. Jacob, private communication, 1994). By using Jacob and Wofsy's data to fit the absorptivity constants, we implicitly assume an effective NO_2/NO_x ratio, stomatal resistance, and cuticle resistance for all biomes equal to those measured during the NASA atmospheric boundary layer experiment 2B in Brazil. An effective rain forest NO_2/NO_x ratio for all biomes will likely underestimate CR in the more polluted northern hemisphere, where higher O_3 levels will cause a higher NO_2/NO_x ratio. An "effective" value will also lead to errors, because there is a nonlinear relationship between intercanopy NO_2/NO_x ratio and soil-NO_x emission. For example, during pulsing events the NO_2/NO_x ratio would drop due to titration of O_3, and net escape from the canopy would increase [*Jacob and Bakwin*, 1991]. We have not accounted for these effects and consider them sources of uncertainty.

6. Experiments and Sensitivity Studies

We performed five case studies to address the issues posed in section 3.

6.1. Cases 1a, 1b, and 1c: *Above-Canopy Emission*

Case 1a is our best estimate of present soil NO_x emission as a source for tropospheric chemistry modeling. We will discuss the results by biome and elaborate on the importance of agriculture by presenting a regional breakdown of fertilizer use, fertilizer-induced emissions, and total emissions. We will also discuss the importance of this source relative to all other known NO_x sources. Cases 1b and 1c are preindustrial and future (year 2025) scenarios. The preindustrial case is computed by replacing agriculture with the NASA/GISS preindustrial land types, and the future case is computed by raising fertilizer rates to projections of *Lashof and Tirpak* [1990].

6.2. Case 2: *Soil Surface Emission*

We run the present-day model without canopy reduction. This will provide an estimate of "raw" soil production and demonstrate the source's sensitivity to canopy reduction. We will use this case to make comparisons with regional emission estimates made around the world and plot time series of individual grid boxes to illustrate the impact of synoptic scale forcing.

6.3. Case 3: *Biomass Burning Experiment*

We decided not to include biomass burning stimulation in our primary emission function (2) because there are not enough data to make a reliable parameterization. As a case study, however, we make a crude approximation for burning effects in tropical grasslands and woodlands by increasing emissions a factor of 3 for the dry to wet season transitional period, defined as the last dry season month and the first wet season month in each grid box. We used a factor of 3, as

Table 6. Canopy Reduction Factors

Biome	LAI[a] (m^2 m^{-2})	SAI[b] (m^2 m^{-2})	CRF (% Loss=1 - CRF)	Seasonal Period Applied
Temperate (30°-poleward)				
Tundra	2	0.010	0.77	year round
Grassland	3.6	0.018	0.64	year round
Woodland	4	0.020	0.61	fall/winter
Coniferous forests	12	0.036	0.39	year round
Deciduous forests	5	0.025	0.55	fall/winter
Agricultural plants	4	0.032	0.57	growing season (incremental[c])
Tropical (30°N-30°S)				
Grassland (savanna)	4	0.020	0.61	year round
Woodland	4	0.040	0.54	year round
Drought-deciduous forest	5	0.075	0.41	wet season
Rain forest	8	0.120	0.25	year round
Agricultural plants[c]	4	0.032	0.57	year round

[a]Barbour et al. [1987].

[b] Computed by multiplying the stomate/leaf ratios presented by Larcher [1991] by the LAIs.

[c] In temperate agriculture, the first growing season month gets no CRF, the second gets 1/3 CRF, the third gets 2/3 CRF, and the fourth gets 1 CRF. In the tropics, 1/2 CRF is applied year round.

Table 7. Emissions Breakdown by Case in Tg N/yr

	Case 1a	Case 1b	Case 1c	Case 2	Case 3
Temperate (30°-poleward)					
Tundra	0.02	0.02	0.02	0.02	0.02
Grassland	0.34	0.49	0.34	0.52	0.33
Woodland	0.05	0.06	0.05	0.09	0.05
Forests					
Conifers	0.01	0.02	0.01	0.03	0.01
Deciduous	0.03	0.04	0.03	0.04	0.03
Agriculture	1.33	...	2.17	1.82	1.33
Tropical (30°N-30°S)					
Grassland	1.60	1.72	1.60	2.50	2.14
Woodland	0.22	0.24	0.22	0.39	0.29
Forests					
Drought deciduous	0.06	0.08	0.06	0.11	0.06
Rain forest	0.85	0.91	0.85	3.40	0.85
Agriculture	0.92	...	1.52	1.16	0.92
TOTAL	5.45	3.59	6.88	10.20	6.07

opposed to 5 or 10 as observed by *Johansson et al.* [1988], because less than 50% of savanna land is burned annually and the 2-month period may overestimate the duration of increased emissions.

7. Results

We present biome-by-biome and total emission results for all five cases in Table 7 and summarize results by case below. For analysis purposes we consider two global domains, tropical (30°N-30°S) and temperate (30°-poleward.)

7.1. Above Canopy Emission

In reasonable agreement with the earlier global annual sources of 4.7 Tg N by *Muller* [1992] and ~5 Tg N by *Dignon et al.* [1992], our model predicts that annual above-canopy soil emissions (case 1a, Figure 1a) are 5.5 Tg N, with 1.8 and 3.7 coming from temperate and tropical regions, respectively. Globally, our strongest contributors are agriculture, grasslands, and tropical rain forests, accounting for 41%, 35%, and 16% of annual emissions, respectively. Although our pattern of annual emissions (see Figure 1a) is in qualitative agreement with that of *Muller* [1992], it is quite different from that of Dignon et al. [1992], which did not include emissions induced by fertilizer application, did not consider canopy recapture, and was dominated by emissions from tropical rain forests. Pulse fluxes, which we define as all fluxes occurring during a pulse, contribute ~1.3 Tg N, or 24% of the annual source. This is consistent with observations in Mexico that pulse fluxes make up 10-22% of annual emissions [*Davidson*, 1992b].

Of the 1.8 Tg N from temperate zones, agriculture accounts for 72%, or 1.3 Tg N. Looking at Table 8, which has a breakdown of emission and fertilizer use by region, we find that 85% of this occurs in the compact northern hemisphere Metro-Agro-Plexes (MAPs) (1.15 Tg N). "Fertilizer-induced" emission equals, as it should, ~1.8% of applied fertilizer (2.5% minus canopy reduction), with the exception of China and Japan, in which it is less because much of the fertilizer is applied to rice in the south. As seen in Figure 1a, there is a dramatic emission increase in China from the rice

Table 8. Fertilizer Use and Above-Canopy Emissions by Region in tg N/yr

Region	Fertilizer Usage	Fertilizer-Induced Emissions	Total Agricultural Emissions	Total Emissions
Europe/Russia MAP	22.90	0.42	0.60	0.74
China and Japan MAP	19.40	0.20	0.22	0.31
North America MAP	11.33	0.21	0.35	0.48
India	10.28	0.11	0.29	0.39
Africa	2.37	0.04	0.34	1.62
South America	1.44	0.03	0.13	0.90
Australia	0.47	0.03	0.11	0.32

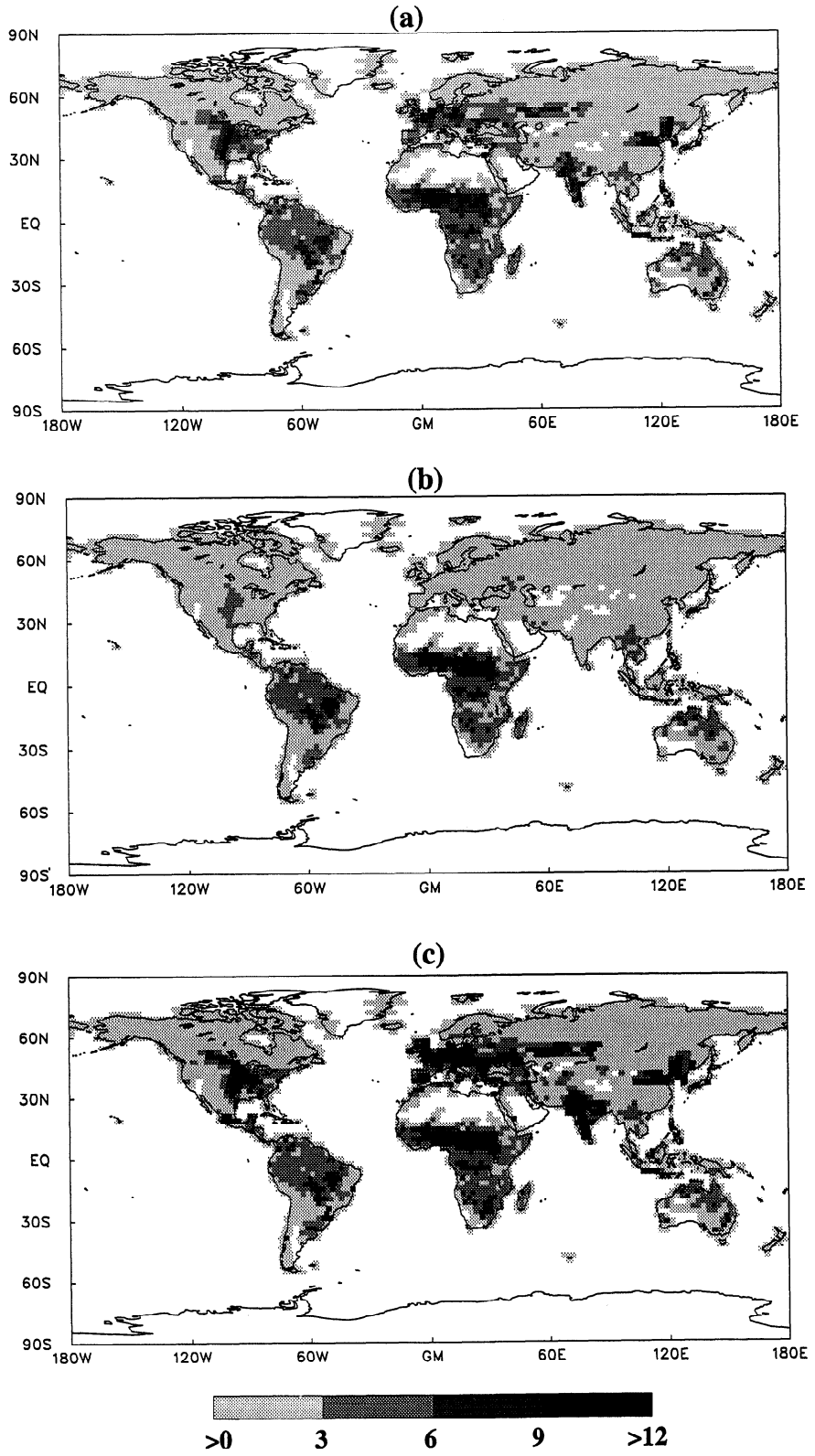

Figure 1. (a) Present, (b) past, and (c) future above-canopy soil-NO_x emissions (mmole N/m^2 yr). The figures are presented on the grid format of the GCM (the Zodiac irregular grid).

fields below 35°N to the millet and wheat fields above 35°N. Based on our fertilizer rate data for China, 190 kg N/ha year, our model predicts that soils above 35°N emit ~45 ng N/m^2 s during the growing season, a level among the highest recorded in the world. Similarly high emissions are also predicted from Europe, where heavy fertilizer use is common. Natural biomes 30°-poleward are less important; grasslands contribute 0.34 Tg N, whereas forests and tundra combined contribute a modest 0.04 Tg N, despite their huge landmass. It is interesting to note that the overall importance of the MAPs are enhanced because 50% of temperate grasslands lie within them. Summing the "total emissions" column in Table 8 results in a net MAP emission of 1.51 Tg N, or 84% of all temperate emissions (both hemispheres). In the tropics (3.65 Tg N), emissions are strong because year-round warmth stimulates vast savannas and rain forests, as well as scattered but not insignificant agriculture. Not surprisingly, our model generates three quarters of global pulsing emissions here, suggesting that tropical ITCZ migration allows a greater amount of land to dry out thoroughly before wetting than do midlatitudes transient disturbances. The most important tropical biome is savanna grassland, which accounts for 1.6 Tg N, or 44% of all tropical soil-biogenic NO_x. Of that, more than half comes from the large belt of African savannas between 0°-20°N, the single largest continental-scale contributor in the world. Tropical agriculture is less important, responsible for only 25% (as opposed to 75% of temperate emissions), and in actuality is much less important from an anthropogenic point of view. With the exception of India, fertilizer use in the 30°N-30°S zone (looking back at Table 8) is so low that most "agriculture" simply emits like natural grasslands. The last important tropical source is rain forests, contributing 23% despite a high rate of canopy reduction. Our conclusion that tropical rain forests do not dominate the above-canopy soil-NO_x budget differs from that of *Dignon et al.* [1992], because their calculations do not include canopy uptake of NO_x.

Preindustrial emissions (Case 1b, Figure 1b) are confined mainly to the tropics. The global integral, 3.6 Tg N, is actually less than would be derived if all fertilizer was removed in the present scenario, because in the process of agricultural development, low-emitting forests were converted into higher-emitting grasslands and pastures. One interesting note: The rice development of southeast Asia actually decreased emissions slightly from preindustrial times. By 2025 (Figure 1c), increasing use of nitrogen fertilizers may almost double preindustrial emissions to 6.9 Tg N. Developing areas such as India and Africa will experience the largest increases, as seen in the figure.

The present contribution of soil-NO_x to the total NO_x budget can be quite significant. To show this, we plot the annual and summer ratios of the case 1 soil-biogenic source to the total NO_x source [*Moxim et al.*, 1994; *Galloway et al.*, 1994] in Figure 2. The total source includes fossil-fuel combustion, biomass burning, biogenic emissions, lightning, stratospheric injection, and aircraft injection, and is computed as a total column sum. Annually, our model predicts that the biogenic source dominates in remote and agricultural regions. The three regions where the soil component is the largest (between 60% and 75%), i.e., western Iran, Australia, and Mongolia, correspond to remote grasslands which are neither cultivated nor densely populated. The reason for the high percentages is not so much large biogenic emissions but rather minuteness of the other sources, particularly the fossil-fuel combustion source. The most important features of Figure 2 are the maximums which appear in the Metro-Agro-Plexes of the northern hemisphere, especially in the midwest United States and southern Russia, where soil emissions annually contribute up to 50% of the NO_x source. In China, the soil-NO_x contribution in the northern grain regions is slightly less than the other MAPs because the high population density of the regions drives up the fossil fuel combustion component. Regarding only July, when conditions are best for ozone formation in the northern hemisphere, soil contributions in remote regions of the MAPs reach 75%, indicating a possible connection between fertilizing and local ozone pollution (discussed more thoroughly by *Chameides et al.* [1994]). In the tropics, the influence of the ITCZ is especially evident in Africa. The potent wet season savannas in the northern hemisphere account for over 75% of that region's total NO_x source, whereas the lower-emitting dry season savannas in the southern hemisphere account for only 15%. This large difference is enhanced by the inverse seasonality of the biomass burning NO_x source (direct NO_x emissions from fire, not to be confused with burning stimulation of biogenic emissions), which is strongest during the dry season, when the biogenic source is weak.

7.2. Soil Surface Emission

In case 2 (Figure 3) we omitted canopy reduction, thus computing an estimate of "raw" soil production. Our below-canopy global source jumps from 5.5 to 10.2 Tg N, indicating that, on average, CR consumes ~50% of annual soil-NO_x emissions. Our calculation of 10.2 Tg N (~9 Tg N if the direct impact of fertilizer application is excluded) is significantly larger than the earlier estimate of 6.6 Tg N by *Muller* [1992] for total below-canopy emission and the earlier estimate of ~5 Tg N by *Dignon et al.* [1992] for natural below-canopy emission. In terms of "raw" surface emission, rain forests are now the dominant source globally, emitting 3.4 Tg N, followed by grasslands and agriculture, each emitting 3 Tg N. As seen by comparing Figures 1a and 3, most canopy reduction occurs in the rain forests of South America and Africa. Remembering that most field measurement techniques exclude canopy reduction, we are able to make comparisons of our below-canopy source with other inventories and experimentally determined budgets around the globe (See Table 9). Our model, with a raw U.S. emission of 0.37 Tg N, is in good agreement with *Williams et al.'s* [1992b] U.S. calculation of 0.31 Tg N. We get similarly good results in comparison with several agricultural fields in the United States and from a countrywide budget prepared for the United Kingdom, as seen in Table 9. Our worst comparison is in the Venezuelan savanna, where we estimate emission rates to be 0.175 g/m^2/year, only 60% of what was estimated by *Johansson et al.* [1988]. However, this comparison is not bad, because our parametrization was fit to extremely variable savanna measurements (looking back at Tables 4 and 5, we see *Johansson et al.'s* [1988] site had clearly the largest emissions measured from savannas to date). Overall, we should expect some agreement with field budgets, because we fit our model with the very same data, but the generally good comparisons (within 40%) indicate that our biome

classification scheme is appropriate at this resolution and that the model climatology is reasonably accurate.

In Figure 4, we plotted several grid boxes of the case 2 data as time series to better illustrate the source's temporal resolution. Figure 4a is in southern Africa (Namibia), where the SAFARI-92 expedition was held to study trace gas emissions and atmospheric chemistry. Researchers there observed elevated biogenic NO_x emissions (20-40 ng N/m^2 s) from a several-hundred-square-kilometer section of the Namibian savanna after a light rainfall at the end of the dry season [*Harris et al.*, 1993]. When similar savannas in South Africa were not pulsing, researchers measured fluxes of 5-12 ng N/m^2 s from wet soils and 1-2 ng N/m^2 s] from dry soils [*Levine et al.*, 1993]. Our model is able to reproduce these observed emission trends quite well. Looking at Figure 4a, we see that peak emissions of 30-50 ng N/m^2 s occur during the larger pulses, whereas emissions from wet and dry soils fluctuate between 5-8 Ng n/m^2 s and 2-3 ng N/m^2 s, respectively. Furthermore, several large pulses occur, as they should, at the end of the dry season (October-November). Figure 4b is a grid box in the agricultural belt of the midwest United States and shows a clear seasonality of emissions as well as rather drastic synoptic scale fluctuations resulting from passing midlatitude disturbances. The annual time series is in good agreement with *Williams et al.* [1988] and *Valente and Thornton* [1993], reaching a peak of 27 ng N/m^2 s in the summer and then dropping off rapidly with the onset of fall and winter. The daily fluctuations of up to 20 ng N/m^2 s are a result of our temperature dependence function ($e^{0.103*T}$), which implies a threefold increase in emission with every 10° increase in soil temperature. As demonstrated by the figure, strongest emissions in temperate climates are likely

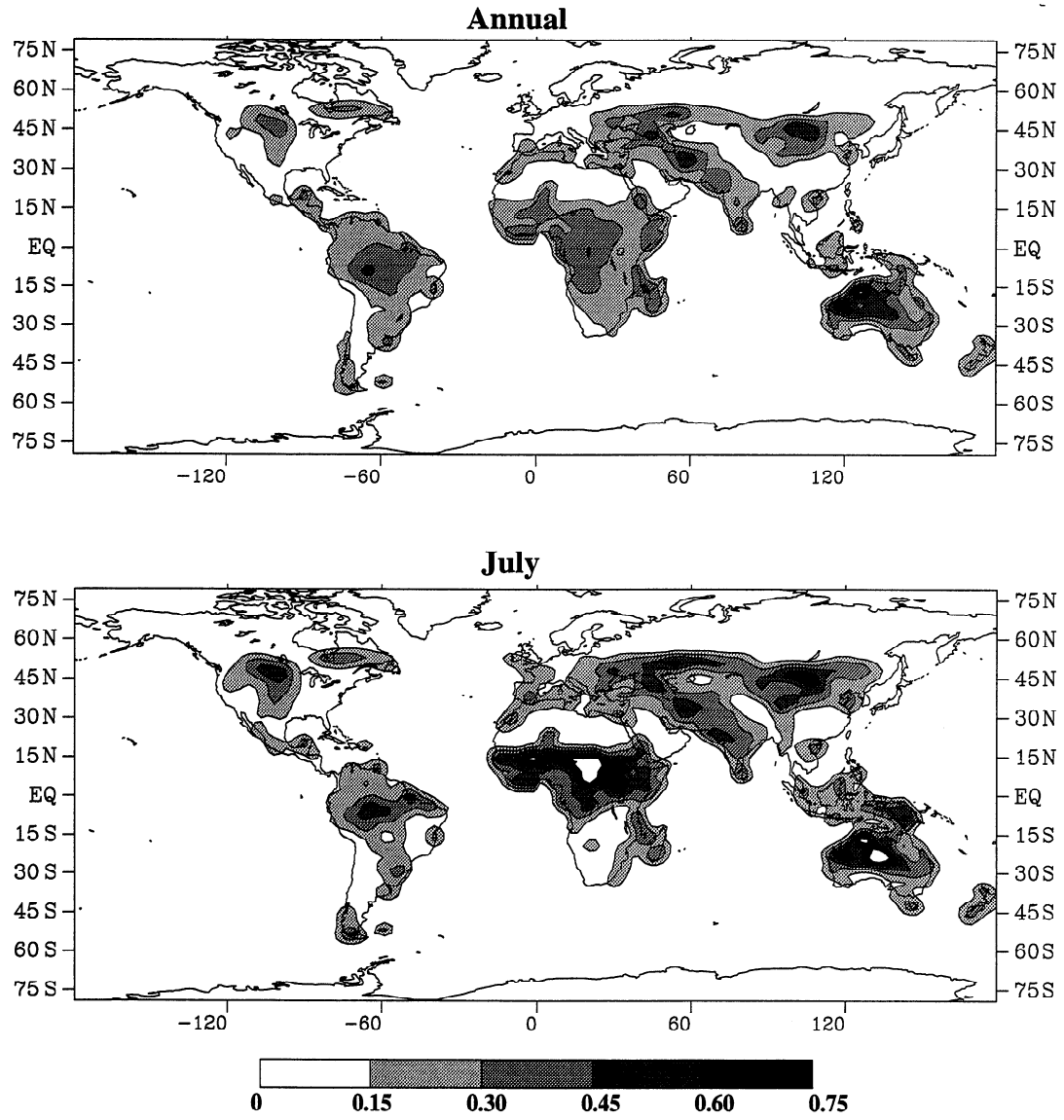

Figure 2. Ratio of soil NO_x emissions to the total NO_x source. The three NH-MAPs are clearly demarcated, as are the potent savannas in the tropics.

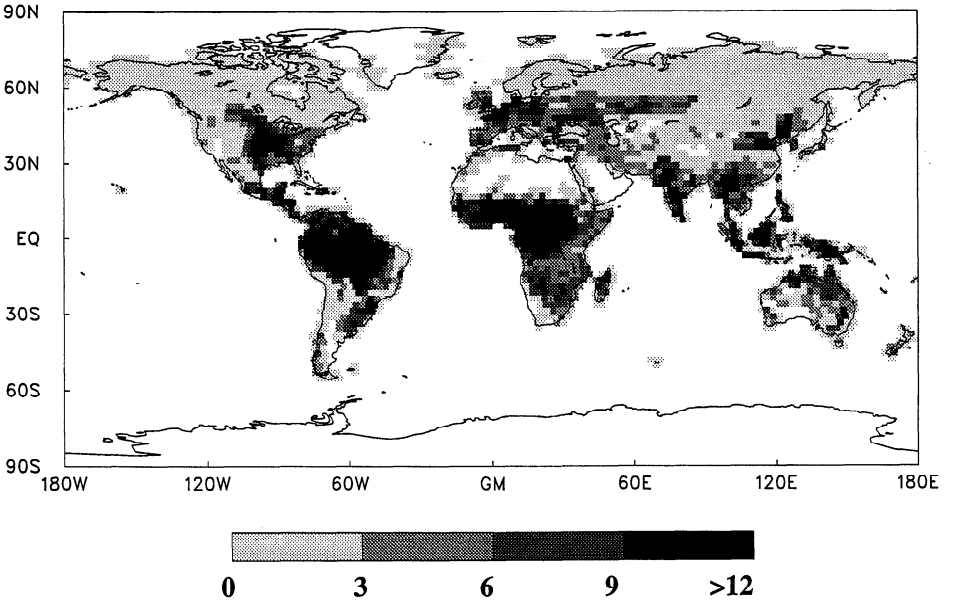

Figure 3. Present "raw" soil NO_x emissions directly from the soil surface (mmole N/m^2 yr). Notice the dominance of the Brazilian and African rain forests when canopy reduction is not considered.

associated with a cycle of warm summertime weather events (typically, stagnant high-pressure systems), which are themselves highly conducive to O_3/smog formation. This correlation promotes high reaction efficiency of net emitted NO_x, and photochemical models using a biogenic NO_x source with only monthly-averaged temperature data will probably underestimate the impact of episodic NO_x emission on photochemical activity. Source sensitivity, computed as the percent difference between emissions computed with 6-hour forcing and monthly averaged forcing, is about 6% globally and 13% in the more dynamic temperate zones.

7.3. Biomass Burning Stimulation

We estimate that biomass burning stimulation may increase tropical savanna and woodland emissions annually by ~0.6 Tg N. In the tropics, we attempted to quantify the net burning stimulation and pulsing effect by summing pulse fluxes that occurred during the dry to wet season transition and adding them to the burning-induced fluxes. We were unable, however, to get an accurate pulse flux estimate, because the transition point varied dramatically between boxes and there was no systematic way to capture it.

Table 9. Comparison of Simulated Soil Surface Emission and Field Data

Site	Period	Experimental Emission Rate, g N m^{-2}	Simulated Emission Rate, g N m^{-2}
Texas grass [a](fertilized with 52kg N/ha)	9 weeks (summer)	0.069-0.237	0.135
Iowa[b]	summer (June-August)	0.145	0.134
South Dakota[b]	summer (June-August)	0.077	0.098
Venezuelan savanna[c]	annual	0.300	0.175
Mexican drought-deciduous forest[d]	annual	0.072	0.045
Virginia cropland[e]	annual	0.208	0.234
U.K.[f]	annual	0.08-0.18	0.165

[a]Hutchinson and Brams [1992].
[b]Williams et al. [1992b] - taken from their Table 5.
[c]Johansson et al. [1988].
[d]Davidson et al. [1991] - experimental rate is average of two sites.
[e]Anderson and Levine [1987].
[f]Skiba et al. [1992].

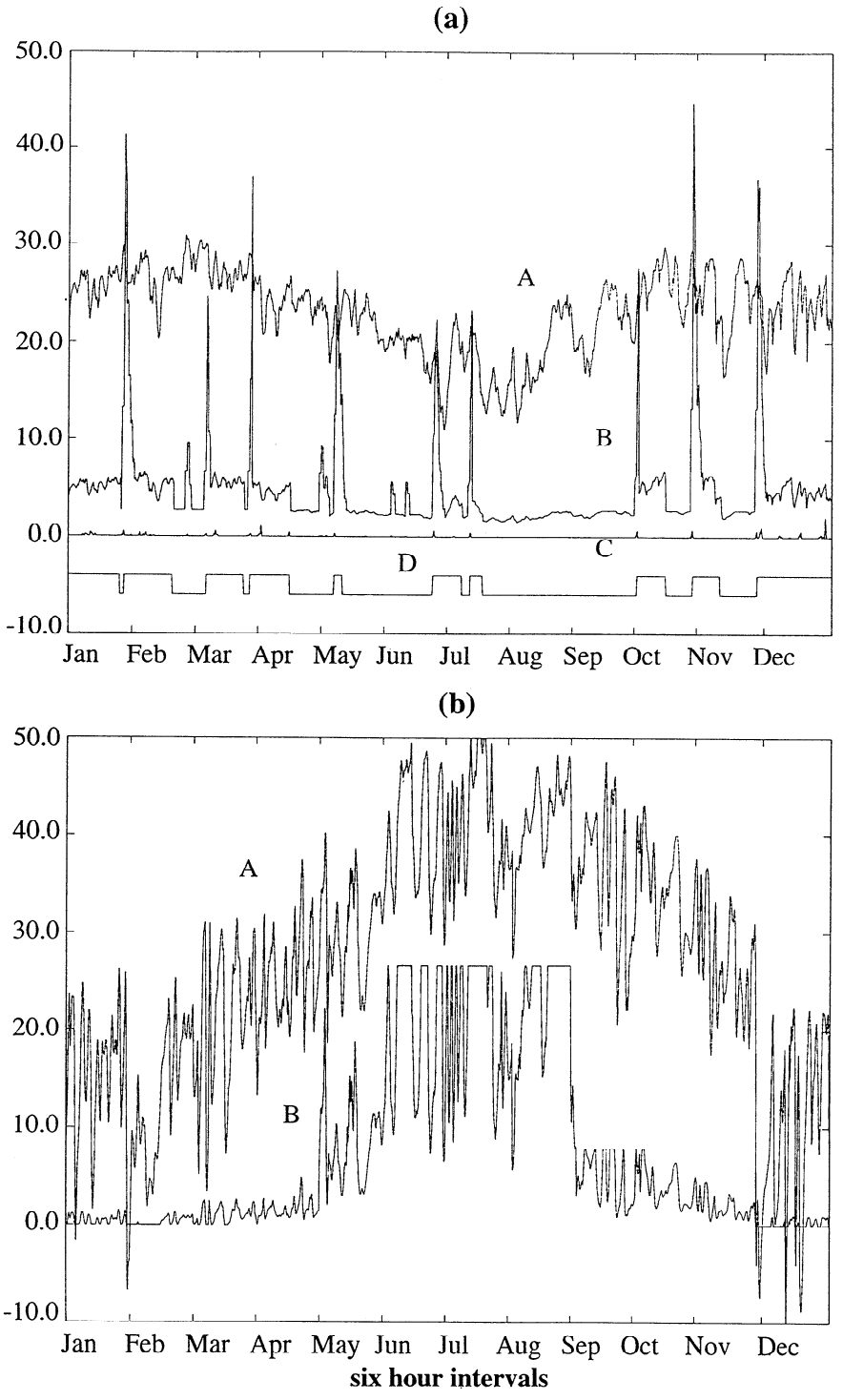

Figure 4. Time series plots of soil NO_x emissions for individual grid boxes. (a) northern Nambia: *A* is air temperature in degrees Celsius, *B* is soil NO_x flux (ng N/m^2 s), *C* is precipitation in centimeters, and *D* represents the soil moisture state [up for "wet," down for "dry"]. (b) midwestern U.S.: *A* is air temperature + 15 in degrees Celsius, and *B* is the soil NO_x flux (ng N/m^2 s).

However, on the basis of the work of *Davidson et al.* [1991] in Mexico, we can estimate that half of all savanna and woodland pulse emissions (~0.4 Tg N) occur somewhere during the 2-month wet/dry season transition described for biomass burning. Therefore aggregate burning stimulation and pulsing effects would produce ~1.0 Tg N, or 40% of annual tropical grassland and woodland emissions, during the relatively short dry to wet season transitional period. We must note that this estimate does not include enhanced emissions from forests that were burned to create agricultural land. *Keller et al.* [1993] showed that these so-called "slash and burn" areas have elevated emissions for several years

following burning, regardless of whether or not they are fertilized. If their results are confirmed by further research, it is possible that we somewhat underestimate the tropical emission budget, because a sizable portion of the rain forests are converted to agriculture each year.

8. Uncertainties and Errors

The empirical nature of this source and the relatively limited quantity of data necessitate that the reader view the source with a certain level of caution. Assessing an exact "confidence" to our numbers is nearly impossible, since, no doubt, they will be modified as new data become available. However, within the constraints of existing data, and as a soil-NO_x source for the current atmospheric chemistry modeling initiatives, this is a useful "best guess." That it reproduces local emission budgets within 50% is promising.

Considering the preindustrial and no-canopy reduction cases as limits, we present an annual soil NO_x emission range of 3.33-10.2 Tg N-N (NO_x)/year. Within this range, the biggest biome-related uncertainties are associated with agriculture and tropical grasslands. The extreme spatial variability of tropical grassland data, coupled with the biome's large areal extent, makes the only 10 or so global data sites vastly inadequate for making a reliable parameterization. This biome requires many more data and another parameter, such as soil nutrients, to better resolve the spatial variability. Agricultural soils have less experimental variability, but field data are limited mainly to North America. The lack of data from other regions is a severe constraint on assessing the confidence of our overall agricultural emission estimate, because they account for 70% of all agricultural emissions. Furthermore, our agricultural modeling does not resolve different cropping practices. Some crops receive much more fertilizer than others (for example, in the United States, corn receives 10 times as much fertilizer as wheat) [*Williams et al.*, 1992b], and sometimes fertilization does not coincide with the growing season. Some fields are fertilized after harvesting, and still others are fertilized on an irregular, nonannual cycle.

Scheme-related uncertainties, such as those from pulsing and canopy reduction, were discussed following the derivation of each scheme. For quantitative uncertainty analysis, there are no data with which to compare our canopy reduction results, but we do get good agreement between our "pulse" flux estimate and the one available measurement in Mexico, as mentioned in section 7. Although no conclusions about uncertainty can be made with just one result, it is at least encouraging. We must add that this study does not include the possibility of pulsing in arid scrubland/desert regions, since we set them to always have zero emission. These areas, which on average have very small fluxes, might provide significant short-term pulses when wetted.

9. Conclusion

This is the first global soil-NO_x source to resolve emission on a synoptic scale and include schemes to simulate pulsing, biomass burning stimulation, canopy reduction, and exhalation of NO_x from nitrogen fertilized soils. Although considerable uncertainties exist, individual site comparisons with experimentally derived budgets generally agree within 50% or better, which is reasonable for this resolution. Key results include the following:

1. Agriculture, specifically the northern hemisphere Metro-Agro-Plexes, dominates soil emission in temperate regions (30°-poleward), whereas grasslands dominate in tropical regions (30°N-30°S).

2. Anthropogenic land use is having a significant impact on global soil-NO_x emission, and it is likely that this trend will continue, given the expected increase in nitrogen fertilizer use. Present NO_x contribution from fertilizers is ~2 Tg N annually.

3. Annually, soil emissions can account for 50% of the total NO_x budget in the tropics and remote agriculture regions in the northern hemisphere. In July, these percentages rise to more than 75%.

4. Stimulation of dry soils by rain, or "pulsing," contributes ~1.3 Tg N annually.

5. Our simplified canopy reduction scheme indicates that, on average, ~50% of soil NO_x emitted at the surface may be deposited on plant and soil surfaces while in transit through the plant canopy. In particular, the impact of emissions from tropical rain forests is sharply reduced from 35% of the "raw" global surface source to 16% of the above-canopy global source.

6. Tropical biomass burning may stimulate an additional 0.6 Tg N (NO_x) emission annually.

7. There are three regions where field research would be most useful: the north African savannas, the agricultural fields of Europe, and northern China. These regions collectively represent ~40% of the total biogenic NO_x and yet have few or no data.

This source will be used in future experiments at GFDL and is available to the general scientific community on a 1° × 1° grid.

Acknowledgments. The authors wish to thank Tony Broccoli, Robbie Toggweiler, Daniel Jacob, Bill Chameides, Prasad Kasibhatla, Bud Moxim and three anonymous reviewers for their helpful comments. We also wish to thank Dave Stocker and Bill Massman for further interpreting their field results for us. We are especially grateful to Dominique Serca for providing us with valuable prepublished African emission data and to Bud Moxim for providing us with an excellent graphic analysis package. This paper is funded by a grant/cooperative agreement from the National Oceanic and Atmospheric Administration (grant NA26RG0102-01). The views expressed herein are those of the authors and do not necessarily reflect the views of NOAA or any of its subagencies.

References

Anderson, I. C., and J. S. Levine, Simultaneous field measurements of biogenic emissions of nitric oxide and nitrous oxide, *J. Geophys. Res.*, *92*, 965-976, 1987.

Anderson, I. C., J. S. Levine., M. A. Proth, and P. J. Riggan, Enhanced biogenic emissions following surface biomass burning, *J. Geophys. Res.*, *93*, 3893-3898, 1988.

Bakwin, P. S., S. C. Wofsy, S.-M. Fan, M. Keller, S. E. Trumbore, and J. M. Da Costa, Emission of nitric oxide from tropical forest soils and exchange of NO between the forest canopy and atmospheric boundary layers, *J. Geophys. Res.*, *95*, 16,755-16,764, 1990.

Bakwin, P. S., S. C. Wofsy, S.-M. Fan, and D. R. Fitzjarrald, Measurements of NO_x and NO_y concentrations and fluxes over arctic tundra, *J. Geophys. Res.*, *97*, 16,545-16,557, 1992.

Barbour, M. G., J. H. Burk, and W. D. Pitts, *Terrestrial Plant Ecology*, edited by Andrew Crowley and Julie Kranhold, p. 278, Benjamin-Cummings, Menlo Park, Calif., 1987.

Cardenas, L., A. Rondon, C. Johansson, and E. Sanhueza, Effects

of soil moisture, temperature, and inorganic nitrogen on nitric oxide emissions from acidic tropical savannah soils, *J. Geophys. Res.*, *98*, 14,783-14,790, 1993.

Chameides, W. L., and J. C. G. Walker, A photochemical theory of tropospheric ozone, *J. Geophys. Res.*, *78*, 8751-8760, 1973.

Chameides, W. L., P. S. Kasibhatla, J. J. Yienger, H. Levy II, and W. J. Moxim, The growth of continental-scale Metro-Agro-Plexes, regional ozone pollution, and world food production, *Science*, *264*, 74-78, 1994.

Chameides, W. L., D. D. Davis, M. O. Rogers, J. Bradshaw, and S. Sandholm, Net ozone photochemical production over the eastern and central north Pacific as inferred by GTE/CITE 1 observations during Fall 1983, *J. Geophys. Res.*, *92*, 2131-2152, 1987.

Crutzen, P. J., Photochemical reaction initiated by and influencing ozone in unpolluted tropospheric air, *Tellus*, *26*, 45-55, 1974.

Crutzen, P. J., The role of NO and NO_2 in the chemistry of the troposphere and stratosphere, *Annual Rev. Earth Planet. Sci.*, *7*, 443-472, 1979.

Davidson, E. A., Sources of nitric oxide and nitrous oxide following the wetting of dry soil, *Soil Sci. Soc. Am. J.*, *56*, 95-102, 1992a.

Davidson, E. A., Pulses of nitric oxide and nitrous oxide following the wetting of dry soil: An assessment of probable sources and importance relative to annual fluxes, *Ecol. Bull.*, *42*, 149-155, 1992b.

Davidson, E. A., P. M. Vitousek, P. A. Matson, and R. Riley, Soil emissions of nitric oxide in a seasonally dry tropical forest of mexico, *J. Geophys. Res.*, *96*, 15,439-15,445, 1991.

Davidson, E. A., P. A. Matson, P. M. Vitousek, R. Riley, K. Dunkin, G. Garcia-Mendez, and J. M. Maass, Processes regulating soil emissions of NO and N_2O in a seasonally dry tropical forest, *Ecology*, *74*, 130-139, 1993.

Delany, A. C., D. R. Fitzjarrald, D. H. Lenschow, R. Pearson, Jr., G. J. Wendel, and B. Woodruff, Direct measurements of nitrogen oxides and ozone fluxes over grassland, *J. Atmos. Chem.*, *4*, 429-444, 1986.

Dignon, J., J. E. Penner, C. S. Atherton, and J. J. Walton, Atmospheric reactive nitrogen: A model study of natural and anthropogenic sources and the role of microbial soil emissions, paper presented at CHEMRAWN VII World Conference on Atmospheric Chemistry, Baltimore, Maryland, 1992.

Fishman, J., S. Solomon, and P. J. Crutzen, Observational and theoretical evidence in support of a significant in situ source of tropospheric ozone, *Tellus*, *31*, 432-446, 1979.

Galbally, I. E., and C. R. Roy, Loss of fixed nitrogen from soils by nitric oxide exhalation, *Nature*, *275*, 734-735, 1978.

Galbally, I. E., J. R. Freney, W. A. Muirhead, J. R. Simpson, A. C. F. Trevitt, and P. M. Chalk, Emissions of nitrogen oxides from a flooded soil fertilized with urea: Relation to other nitrogen loss processes, *J. Atmos. Chem.*, *5*, 343-365, 1987.

Galloway, J. N., H. Levy II, and P. S. Kasibhatla, Year 2020: Consequences of population growth and development on deposition of oxidized nitrogen, *Ambio*, *23*, 120-123, 1994.

Hameed, S., and J. Dignon, Changes in the geographical distributions of global emissions of NO_x and SO_x from fossil-fuel combustion between 1966 and 1980, *Atmos. Environ.*, *22*, 441-449, 1988.

Hanson, P. J., and S. E. Lindberg, Dry deposition of reactive nitrogen compounds: A review of leaf, canopy and non-foliar measurements, *Atmos. Environ.*, *25A*, 1615-1634, 1991.

Hao, W. M., M. H. Liu, and P. J. Crutzen, Estimates of annual and regional releases of CO_2 and other trace gases to the atmosphere from fires in the tropics, based on FAO statistics from the period 1975-1980, in *Fire in the tropical biota: Ecosystem processes and global challenges*, edited by J. G. Goldammer, Ecological Studies 84, pp. 440-462, Springer-Verlag, Berlin-Heidelberg, 1990.

Harris, G. W., T. Zenker, F. G. Wienhold, M. Welling, and U. Parchatka, Airborne observations of strong biogenic NO_x emissions from the Namibian savanna at the end of the dry season (abstract), *EOS Trans. AGU*, *74(43)*, Fall Meeting Suppl., 118, 1993.

Hutchinson, G. L., and E. A. Brams, NO versus N_2O emissions from an NH_4^+-amended Bermuda grass pasture, *J. Geophys. Res.*, *97*, 9889-9896, 1992.

Jacob, D. J., and P. S. Bakwin, Cycling on NO_x in tropical forest canopies, in *Microbial Production and Consumption of Greenhouse Gases: Methane, Nitrogen Oxides, and Halomethanes*, edited by J. E. Rogers and W. B. Whitman, pp. 237-253, American Society of Microbiology, Washington, D.C., 1991.

Jacob, D. J., and S. C. Wofsy, Budgets of reactive nitrogen, hydrocarbons, and ozone over the Amazon rain forest during the wet season, *J. Geophys. Res.*, *95*, 16,737-16,754, 1990.

Johansson, C., Field measurements of emissions of nitric oxide from fertilized and unfertilized forest soils in Sweden, *J. Atmos. Chem.*, *1*, 429-442, 1984.

Johansson, C., and E. Sanhueza, Emission of NO from savannah soils during rainy reason, *J. Geophys. Res.*, *93*, 14,193-14,198, 1988.

Johansson, C., H. Rodhe, and E. Sanhueza, Emission of NO in a tropical savanna and a cloud forest during the dry season, *J. Geophys. Res.*, *93*, 7180-7192, 1988.

Kaplan, W. A., S. C. Wofsy, M. Keller, and J. M. Da Costa, Emission of NO and deposition of O_3 in a tropical forest system, *J. Geophys. Res.*, *93*, 1389-1395, 1988.

Kasibhatla, P. S., NO_y from sub-sonic aircraft emissions: A global three-dimensional model study, *Geophys. Res. Lett.*, *20*, 1707-1710, 1993.

Kasibhatla, P. S., H. Levy II, W. J. Moxim, and W. L. Chameides, The relative impact of stratospheric photochemical production on tropospheric NO_y levels: A model study, *J. Geophys. Res.*, *96*, 18,631-18,646, 1991.

Keller, M., E. Veldkamp, A. M. Weitz, and W. A. Reiners, Effect of pasture age on soil trace-gas emissions from a deforested area of Costa Rica, *Nature*, *365*, 244-246, 1993.

Larcher, W., *Physiological Plant Ecology*, p. 91, Springer-Verlag, New York, 1991.

Lashof, D. A., and D. A. Tirpak, *Policy Options for Stabilizing Global Climate*, Hemisphere, New York, 1990.

Levine, J. S., W. R. Cofer III, D. I. Sebacher, R. P. Rhinehart, E. L. Winstead, S. Sebacher, C. R. Hinkle, P. A. Schmalzer, and A. M. Koller Jr., The effects of fire on biogenic emissions of methane and nitric oxide from wetlands, *J. Geophys. Res.*, *95*, 1853-1864, 1990.

Levine, J. S., W. R. Cofer III, D. R. Cahoon, D. I. Sebacher, E. L. Winstead, M. C. Scholes, D. Parsons, and R. J. Scholes, Biogenic emissions of nitric oxide and nitrous oxide from the savanna grasslands of southern Africa (abstract), *EOS Trans. AGU*, *74(43)*, Fall Meeting Suppl., 118, 1993.

Levy, H. II, Normal atmosphere: Large radical and formaldehyde concentrations predicted, *Science*, *173*, 141-143, 1971.

Levy, H. II, and W. J. Moxim, Simulated global distribution and deposition of reactive nitrogen emitted by fossil fuel combustion, *Tellus*, *41*, 256 - 271, 1989.

Levy, H. II, J. D. Mahlman, and W. J. Moxim, A stratospheric source of reactive nitrogen in the unpolluted troposphere, *Geophys. Res. Lett.*, *7*, 441-444, 1980.

Levy, H. II, W. J. Moxim, P. S. Kasibhatla, and J. A. Logan, The global impact of biomass burning on tropospheric reactive nitrogen, in *Global Biomass Burning: Atmospheric, climatic, and biospheric implications*, edited by J. S. Levine, p. 363-369, MIT Press, Cambridge, Mass., 1991.

Lin, X., M. Trainer, and S. C. Liu, On the nonlinearity of the

tropospheric ozone production, *J. Geophys. Res.*, *93*, 15,879-15,888, 1988.

Logan, J. A., Nitrogen oxides in the troposphere: Global and regional budgets, *J. Geophys. Res.*, *88*, 10,785 - 10,807, 1983.

Manabe, S., and J. L. Holloway Jr., The seasonal variation of the hydrologic cycle as simulated by a global model of the atmosphere, *J. Geophys. Res.*, *80*, 1617-1649, 1975.

Manabe, S., D. G. Hahn, and J. L. Holloway Jr., The seasonal variation of the tropical circulation as simulated by a global model of the atmosphere, *J. Atmos. Sci.*, *31*, 43-83, 1974.

Mathews E., Global vegetation and land use: New high resolution data bases for climate studies, *J. Clim. Applied Meteorol.*, *22*, 474-486, 1983.

Mathews E., Atlas of archived vegetation, land-use, and seasonal albedo data sets, *NASA Tech. Memo 86199*, 1985.

Matson, P. A., C. R. Billow, and S. Hall, Fertilization practices in tropical sugar cane systems affect nitrogen trace gas fluxes (abstract), *EOS Trans. AGU*, *74(43)*, Fall Meeting Suppl., 136, 1993.

Menaut, J.-C., L. Abbadie, F. Lavenu, P. Loudjani, and A. Podaire, Biomass burning in west Africa savannas, in *Global Biomass Burning: Atmospheric, Climatic, and Biospheric Implications*, edited by J. S. Levine, pp. 133-142, MIT Press, Cambridge, Mass., 1991.

Moxim, W. J., H. Levy II, P. S. Kasibhatla, and W. L. Chameides, The impact of anthropogenic and natural NO_x sources on the global distribution of tropospheric reactive nitrogen and the net chemical production of ozone (abstract), *EOS Trans. AGU*, *75*, Fall Meeting Suppl., 135, 1994.

Muller, J.-F., Geographical distribution and seasonal variation of surface emissions and deposition velocities of atmospheric trace gases, *J. Geophys. Res.*, *97*, 3787-3804, 1992.

National Academy of Sciences, *Acid Deposition*, National Academy Press, Washington, D.C., 1983.

National Academy of Sciences, *Rethinking the Ozone Problem in Urban and Regional Air Pollution*, National Academy Press, Washington, D.C., 1991.

Parrish, D. D., E. J. Williams, D. W. Fahey, and F. C. Fehsenfeld, Measurement of nitrogen oxide fluxes from soils: Intercomparison of enclosure and gradient measurement techniques, *J. Geophys. Res.*, *92*, 2165-2171, 1987.

Penner, J. E., C. S. Atherton, J. Dignon, S. J. Ghan, J. J. Walton, and S. Hameed, Tropospheric nitrogen: A three-dimensional study of sources, distributions, and deposition, *J. Geophys. Res.*, *96*, 959-990, 1991.

Rondon, A., C. Johansson, and E. Sanhueza, Emission of nitric oxide from soils and termite nests in a Trachypogon Savanna of the Orinoco Basin, *J. Atmos. Chem.*, *17*, 293-306, 1993.

Sanhueza, E., Biogenic emissions of NO and N_2O from tropical savanna soils, in *Proceedings of International Symposium on Global Climate Change*, pp. 22-34, Japan National Committee for the IGBC, Tokyo, 1992.

Sanhueza, E., W.-M. Hao, D. Scharffe, L. Donoso, and P. J. Crutzen, N_2O and NO emissions from soils of the northern part of the Guayana Shield, Venezuela, *J. Geophys. Res.*, *95*, 22,481-22,488, 1990.

Shepard, M. F., S. Barzetti, and D. R. Hastie, The production of NO_x and N_2O from a fertilized agricultural soil, *Atmos. Environ.*, *25A*, 1961-1969, 1991.

Skiba, U., K. J. Hargreaves, D. Fowler, and K. A. Smith, Fluxes of nitric and nitrous oxides from agricultural soils in a cool temperate climate, *Atmos. Environ.*, *26A*, 2477-2488, 1992.

Slemr, F., and W. Seiler, Field measurements of NO and NO_2 emissions from fertilized and unfertilized soils, *J. Atmos. Chem.*, *2*, 1-24, 1984.

Slemr, F., and W. Seiler, Field study of environmental variables controlling the NO emissions from soil and the NO compensation point, *J. Geophys. Res.*, *96*, 13,017-13,031, 1991.

Stocker, D. W., D. H. Stedman, K. F. Zeller, W. J. Massman, and D. G. Fox, Fluxes of nitrogen oxides and ozone measured by eddy correlation over a shortgrass prairie, *J. Geophys. Res.*, *98*, 12,619-12,630, 1993.

Thornton, F. C., and R. J. Valente, Emissions of nitric oxide from soils on varying land-use types located in the Tennessee Valley, in *Agronomy Abstracts*, p. 262, Madison, Wisc., 1992.

Times Atlas of the World, p. xxvii, Houghton Mifflin, Boston, Mass., 1967.

Trainer, M., et al., Correlations of ozone with NO_y in photochemically aged air, *J. Geophys. Res.*, *98*, 2917-2925, 1993.

Valente, R. J., and F. C. Thornton, Emissions of NO from soil at a rural site in central Tennessee, *J. Geophys. Res.*, *98*, 16,745-16,753, 1993.

Williams, E. J., and F. C. Fehsenfeld, Measurement of soil nitrogen oxide emissions at three North American ecosystems, *J. Geophys. Res.*, *96*, 1033-1042, 1991.

Williams, E. J., D. D. Parrish, and F. C. Fehsenfeld, Determination of nitrogen oxide emissions from soils: Results from a grassland site in Colorado, United States, *J. Geophys. Res.*, *92*, 2173-2179, 1987.

Williams, E. J., D. D. Parrish, M. P. Buhr, F. C. Fehsenfeld, and R. Fall, Measurement of soil NO_x emissions in central Pennsylvania, *J. Geophys. Res.*, *93*, 9539-9546, 1988.

Williams, E. J., G. L. Hutchinson, and F. C. Fehsenfeld, NO_x and N_2O emissions from soils, *Global Biogeochem. Cycles*, *6*, 351-388, 1992a.

Williams, E. J., A. Guenther, and F. C. Fehsenfeld, An inventory of nitric oxide emissions from soils in the United States, *J. Geophys. Res.*, *97*, 7511-7519, 1992b.

H. Levy II (corresponding author) and J. J. Yienger, Geophysical Fluid Dynamics Laboratory, Princeton University, P.O. Box 308, Princeton, NJ 08542. (e-mail: hl@gfdl.gov)

(Received May 31, 1994; revised January 14, 1995; accepted January 14, 1995.)